Received: 8 February 2023 | Revised: 5 December 2023 | Accepted: 12 January 2024

DOI: 10.1111/obr.13716

REVIEW

OBESITY Reviews WILEY

Ultrasound-based measurement of central adiposity: Key considerations and guidelines

Gabriel Zieff[1,2] | Jon Cornwall[3] | Malia N. Blue[1] | Abbie E. Smith-Ryan[1] | Lee Stoner[1,4]

[1]Department of Exercise and Sport Science, University of North Carolina at Chapel Hill, Chapel Hill, North Carolina, USA

[2]Human Movement Science Curriculum, University of North Carolina at Chapel Hill, Chapel Hill, North Carolina, USA

[3]Centre for Early Learning in Medicine, Otago Medical School, University of Otago, Dunedin, New Zealand

[4]Department of Epidemiology, Gillings School of Public Health, University of North Carolina at Chapel Hill, Chapel Hill, North Carolina, USA

Correspondence
Gabriel Zieff, School of Kinesiology The University of British Columbia, Vancouver, British Columbia, V6T1Z1, Canada.
Email: gabriel.zieff@ubc.ca

Summary

Central adiposity, which is visceral and subcutaneous adiposity in the abdominal region, is a known risk factor for developing chronic cardiometabolic diseases. Central adiposity can be measured relatively inexpensively using ultrasound. Ultrasound has been shown to be precise and reliable, with measurement accuracy comparable to computed tomography and magnetic resonance. Despite the advantages conferred by ultrasound, widespread adoption has been hindered by lack of reliable standard operating procedures. To consolidate the literature and bring clarity to the use of ultrasound-derived measures of central adiposity, this review outlines (i) the [patho] physiological importance of central adiposity to cardiometabolic disease risk; (ii) an overview of the history and main technical aspects of ultrasound methodology; (iii) key measurement considerations, including transducer selection, subject preparation, image acquisition, image analysis, and operator training; and (iv) guidelines for standardized ultrasound protocols for measuring central adiposity.

KEYWORDS
cardiovascular disease risk, central adiposity, guidelines, non-invasive, obesity, standardization, ultrasound

1 | INTRODUCTION

The purpose of this review was to consolidate the literature and bring clarity to the use of ultrasound-derived measures of central adiposity, a known risk factor for cardiometabolic diseases (CMDs).[1–3] Central adipose tissue, defined as excess body adiposity in the abdominal region (including both visceral and subcutaneous adiposity), has traditionally been quantified using computed tomography (CT) and magnetic resonance imaging (MRI).[4,5] Ultrasound is also precise and reliable,[6] with measurement accuracy comparable to computed tomography and magnetic resonance approaches,[4,7]yet with significantly lower cost and risk. Despite the advantages conferred by ultrasound, few guidelines exist to direct users in regard to "best practice" measurement of central adiposity.

The lack of clear guidelines regarding the use of ultrasound-based central adiposity assessments in clinical and research practices hinders efforts to compare outcomes across studies. To fill this gap in the literature, the current review outlines (i) the [patho]physiological importance of central adiposity to CMD risk; (ii) an overview of the history and main technical aspects of ultrasound methodology; (iii) key measurement considerations, including transducer selection, subject preparation, image acquisition, image analysis, and operator training; and (iv) guidelines for standardized ultrasound protocols for measuring central adiposity. Key terms and definitions are provided in Table 1.

2 | CENTRAL ADIPOSITY AND ITS MEASUREMENT

In this section, we first briefly describe the distribution and primary [patho]physiological roles of different central adipose depots in the

TABLE 1 List of key terminology and definitions.

Term	Definition
Abdominal wall fat Index	The ratio of preperitoneal fat thickness to minimum subcutaneous fat thickness.
Attenuation	Phenomenon of acoustic waves losing amplitude and intensity; because of scattering, non-reciprocal wave reflection, and wave absorption.
Body Mass Index	Anthropometric index of body size associated with body composition in large samples, but poor reflection of body composition at the individual level because it does not discern adiposity versus lean mass.
Cardiometabolic disease risk	Risk of chronic cardiovascular (e.g., myocardial infarction) and metabolic (e.g. type II diabetes mellitus) conditions, which share risk factors including obesity.
Central adiposity	Refers to the amount of adipose deposits within the abdominal region; also referred to as visceral adiposity or visceral adiposity.
Computed tomography	Imaging technology involving an X-ray that rotates around a central axis. Can be used for central adiposity measurements. Limited by size, radiation, and cost.
Dual X-ray Absorptiometry	Dual X-ray Absorptiometry; imaging technology involving two X-ray beams with different energy levels. Can be used for central adiposity measurements. Limitations: bulk/size, ionizing radiation, and cost.
Frequency	Number of ultrasound waves/unit time. Dependent on probe type.
Intra-abdominal adiposity thickness	The original ultrasound-based marker of visceral adiposity; measured as the distance between anterior wall of aorta and linea alba. Sometimes referred to as visceral adipose tissue.
Intraclass correlation coefficient	Statistic used to describe the similarity between measurements; can be used for testing measurement reliability and repeatability.
Impedance	The physical resistance that an acoustic waveform encounters, and the product of tissue density × wave propagation speed.
Linea alba	Posterior surface of rectus abdominis muscle
Maximum abdominal ratio	The ratio of intra-abdominal fat thickness to maximum subcutaneous fat thickness.
Magnetic resonance imaging	Imaging technology involving a magnetic field and radio waves. Can be used for central adiposity measurements. Limitations: bulk/size, ionizing radiation, and cost.
Preperitoneal circumference	An indirect measure of the v/s ratio calculated as waist circumference—(2π × subcutaneous fat thickness), where subcutaneous fat thickness is measured at the midpoint between the umbilicus and the xiphoid process on the linea alba.
Maximum preperitoneal adiposity thickness	A measure of visceral adiposity; extends from the anterior surface of the liver (left lobe) to the posterior surface of linea alba.
Piezoelectricity	The principle that materials, when deformed, produce a voltage. With ultrasound, a voltage from the ultrasound deforms probe's piezoelectric crystals resulting in an ultrasound wave.
Maximum subcutaneous adiposity thickness	A measure of subcutaneous adiposity; defined as the thickness of the subcutaneous adiposity between the anterior surface of the linea alba and the adiposity-skin barrier, measured 2 cm above the umbilicus.
Minimum subcutaneous adiposity thickness	A measure of subcutaneous adiposity; defined as the thickness of the subcutaneous adiposity between the anterior surface of the linea alba and the adiposity–skin barrier, measured just below the xiphoid process.
Waist-to-hip ratio	Ratio between waist and hip circumferences.

body. Then we go on to briefly describe the major ultrasound-based measurements of central adiposity.

2.1 | [Patho]physiology

Figure 1 displays anatomical locations of the main adiposity types and depots in the abdominal region. Central adiposity is associated with poor cardiovascular and metabolic health.[3,8] The following subsections describe the anatomical and [patho]physiological properties of three primary depots of central adiposity: intraperitoneal visceral adiposity, preperitoneal visceral adiposity, and subcutaneous adiposity.

2.1.1 | Intraperitoneal visceral adiposity

Intraperitoneal visceral adiposity is the depot of adipose tissue *within* the confines of the peritoneum—the mesothelial membrane surrounding the majority of intra-abdominal organs including the stomach, spleen, and parts of the intestines and liver.[9] The close proximity of adiposity in this region to said organ systems and the shared vascular networks which serve these tissues are thought to contribute to its strong relationship with CMD risk factors including insulin resistance and inflammation.[10] Physiologically, increased free fatty acid exposure in the bloodstream as a result of intraperitoneal visceral adiposity decreases adiposity metabolism and promotes hepatic adiposity deposition.[11] Central adiposity has been associated with a variety of CMD

risk factors including elevated cholesterol,[12] impaired glucose regulation,[13,14] insulin resistance,[10] systemic inflammation,[15] hypertension,[16] and fatty liver.[17] Furthermore, visceral adipocytes release pro-inflammatory cytokines and vasoactive peptides, including interleukin-6, tumor necrosis factor, angiotensin II, and plasminogen activator inhibitor-1, which increase inflammation and impair vascular function.[18]

2.1.2 | Preperitoneal visceral adiposity

Preperitoneal visceral adiposity is deposited outside the peritoneum.[19] This deposit lines the abdominal wall from between the pelvis and umbilicus upwards to the xiphoid process; the actual depot of adipose tissue exists between the linea alba and peritoneum (Figure 1). The thickness of this adipose tissue varies depending on whether the site being considered is more distal and closer to the umbilicus (thicker) or more proximal and closer to the xiphoid process (less thick). Whereas intraperitoneal visceral adipose tissue extrudes to the portal vein, preperitoneal visceral adipose tissue extrudes to the systemic blood circulation rather than the portal vein. Because of these characteristics, some researchers have suggested that preperitoneal adiposity is therefore not visceral adiposity per se,[19,20] while others do refer to this depot as visceral.[19,21,22] We take the latter stance because this adipose depot is adjacent to the main visceral organ responsible for metabolic function—the liver. Some preperitoneal adipose tissue may even be in direct contact with the bare area (superoposterior aspect) of the liver which is not contained within the peritoneum.[9] The proximity of this adiposity compartment to the liver

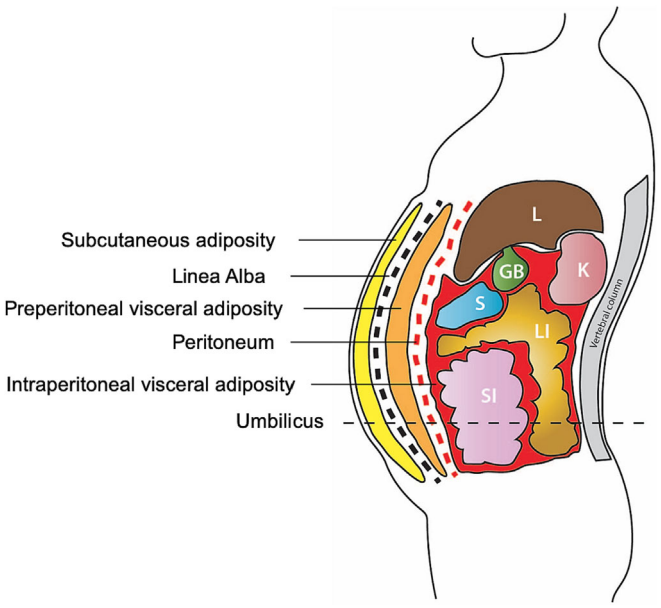

FIGURE 1 Diagram illustrating a sagittal view of the relative locations and sizes of the main central adiposity depots and visceral organs. GB, gallbladder; K, kidney; L, liver; LI, large intestine; S, stomach; SI, small intestine.

may contribute to CMD risk by impairing hepatic glucose and triglyceride metabolism.[23,24]

2.1.3 | Subcutaneous adiposity

Subcutaneous adiposity exists throughout the body, just below the skin layer. In terms of subcutaneous adiposity in the abdominal region, this compartment extends from between the pelvis and umbilicus upwards to the xiphoid process, and is considered the adipose tissue between the anterior surface of the linea alba and the diposity-skin barrier. Like preperitoneal visceral adiposity, thickness of this adipose tissue varies depending on whether the site being considered is more distal and closer to the umbilicus (thicker) or more proximal and closer to the xiphoid process (less thick). While it is accepted that visceral adipose tissue is a major risk factor for cardiometabolic complications, the role of subcutaneous adipose tissue is less clear. For example, subcutaneous adiposity seems to have both protective and CMD-promoting effects, depending on the absolute and relative (to visceral) amount.[2,25] In terms of its protective capacity, subcutaneous adipose tissue can accommodate excess triglycerides and thus may act as a preventive buffer against the flow of lipid into the visceral depot and non-adipose tissues.[26,27] On the other hand, relationships have been reported between excess subcutaneous adiposity and CMD risk factors including low (LDL) and high-density lipoprotein (LHDL), as well as total cholesterol levels, although these relationships do not seem to be as strong as relationships with visceral adiposity.[2,21,23] The amount of visceral adiposity relative to subcutaneous adiposity (v/s ratio) may also be a superior predictor of CMD risk than subcutaneous adiposity alone, with higher ratios corresponding to increased triglycerides, cholesterol, impaired glucose and lipid metabolism, and endothelial dysfunction.[19,28] Collectively, while total and percent body adiposity are important, visceral (i.e., intra- and preperitoneal visceral adiposity) adiposity poses a greater risk for developing CMD risk and obesity-related disorders than overall or subcutaneous adiposity.[2,29,30]

2.2 | Measurement of central adiposity

The capacity for practical, valid, and reliable assessments of central adiposity (intra- and preperitoneal visceral compartments) is noteworthy because it is a key predictor of CMD risk as described above.[16] Relatively simple anthropometric techniques are available for estimating central adiposity such as waist-to-hip ratio, waist circumference, and abdominal sagittal diameter.[1] However, compared to the gold standard, more technical methods such as CT, MRI, and dual X-ray absorptiometry (DXA), anthropometric techniques are not accurate (valid) and have poor precision (reliability).[1,31,32] Alternatively, CT, MRI, and DXA permit highly precise and accurate assessment of central adipose tissue[1,33]; but these techniques require highly technical equipment, are expensive, take considerable time to generate measurements, and have limited accessibility. Furthermore, CT and DXA produce ionizing radiation, making these methods particularly

unsuitable for use on certain populations including children and pregnant females.

Ultrasound is a safe and precise modality that has been well-validated against CT[28,34–42] and MRI for measurement of body adiposity.[7,16,34,35,43–45] Moreover, ultrasound is relatively inexpensive and can be portable, making it suitable for wide-spread adoption among health-care providers and researchers. Although ultrasound is not currently used routinely for central adiposity assessments in clinical settings, there is a substantial body of literature that demonstrates the capacity for ultrasound to be utilized for this purpose.[6,46]

3 | HISTORICAL AND TECHNOLOGICAL OVERVIEW OF ULTRASOUND

In this section, we describe the history and basic tenants of the ultrasound technology facilitating measurement of central adiposity. First, we will describe the historical context of biomedical ultrasound technology generally. Then, we provide broad context to the measurement of central adiposity by briefly outlining the underlying physics which underpin biomedical ultrasound. This background information will help illustrate the scope and utility of ultrasound technology as an effective, dynamic tool in biomedical research and clinical contexts. Moreover, our aim is for this information to enable readers to gain some basic fluency in the fundamental technological principles and physics of ultrasound, including those impacted by user settings and practices.

3.1 | Historical

The use of medical ultrasound began during the second World War in Europe, Japan, and the United States.[47] Pioneering work by Dr. Ian Donald and colleagues in Glasgow during the 1950s showed that ultrasound could reliably identify abdominal masses and treatable pregnancy abnormalities.[47,48] This breakthrough is often viewed as the "turning point" in medical ultrasound, which spurred broader acceptance and investigation of the technology.[47] While widespread ultrasound use has not yet been adopted for assessment of central adiposity, the technology is considered a "staple" for diagnostic and surgical procedures in a variety of other health-care contexts including oncology, obstetrics, and orthopedics. Reflecting its widespread popularity, the global ultrasound market size was valued at $7.9 billion in 2021.[49]

3.2 | Technological

In terms of the underlying physics, ultrasound detects differences in tissues through the transmission and reception of high-frequency pulse echoes or acoustic sound waves (Figure 2). The reflected soundwaves contain spatial and contrast information that allows the construction of a two-dimensional image which is visualized by the user on a screen or display. While there are several "modes" of ultrasound that have been developed and used for various purposes (e.g., A-mode results in one-dimensional waveform with peaks at tissue interfaces[50]; M-mode is used for high temporal resolution view of tissue

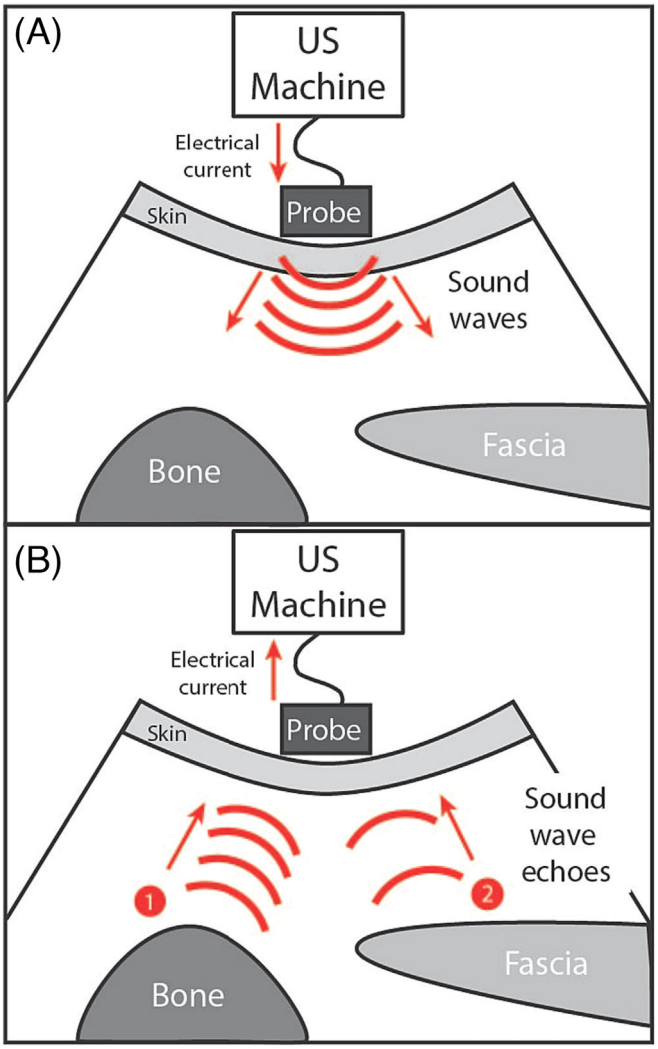

FIGURE 2 Schematic illustrating how ultrasound works using the principle of piezoelectricity and the principle of impedance in ultrasound technology. (A) Ultrasound generated sound waves. Application of an electrical current to the piezoelectric crystals located in the ultrasound probe cause the crystals to vibrate and send ultrasound (acoustic) waves into the body tissue. (B) Return of soundwaves to ultrasound machine, with the principle of impedance illustrated. When acoustic waveforms hit a high-density surface such as bone (B1), they are almost entirely reflected. In contrast, waveforms are more readily absorbed by less dense tissues, such as fascia (B2), which limits the amount of acoustic reflections sent back to the ultrasound probe and machine. Reflected acoustic waves hit the piezoelectric crystals in the probe, causing them to vibrate and generate an electrical current that is returned to, and analyzed by, the ultrasound machine which constructs an image based on the information received. Because there is more soundwave information being returned to the ultrasound machine from more dense tissues that have low impedance, these structures will appear more clearly on ultrasound images than those of less dense tissues which have higher impedance. US, ultrasound.

movement[51]), Brightness (B)-mode, which displays a two-dimensional black and white image, is arguably the most widely used, largely because of good image quality. It is also the most relevant imaging mode in the context of central adiposity assessments because it produces two-dimensional images in real time. Therefore, this review aims to address techniques using B-mode ultrasound.[6,46,52]

There are several principles which are key in understanding the technology and utility of ultrasound imaging. These principles include piezoelectricity, impedance, frequency, and attenuation, each of which will be briefly described below. Readers seeking a more nuanced discussion of ultrasound-related acoustic physics as well as global and probe-dependent settings are directed to resources elsewhere.[53–56]

3.2.1 | Piezoelectricity

Ultrasound transducers transmit their signals through the principle of piezoelectricity, which states that some materials, when deformed, produce a voltage.[54] In the case of ultrasound, a voltage from the ultrasound machine deforms piezoelectric crystals in the ultrasound probe.[53] This causes a pressure that results in an ultrasound waveform that passes out into the tissues the probe is in contact with.[54] The piezoelectric crystals are therefore responsible for converting electrical voltages into ultrasound pulses (mechanical acoustic vibrations). This process also works in reverse to generate ultrasound images, with the soundwave pulses "echoing" back from tissues and causing deformation in the piezoelectric crystals in the ultrasound probe. These pulses are re-converted into voltages which are transmitted back to the ultrasound machine from the probe to be displayed and visualized as images.[53] Figure 2 shows the principle of piezoelectricity in the context of ultrasound technology.

3.2.2 | Impedance

A reflection of the ultrasound beam, or acoustic wave, is called an "echo," with the production and detection of echoes forming the basis of ultrasound. A reflection occurs at the boundary between two materials provided that certain properties of the materials are different.[53] The key property of interest is known as acoustic impedance, defined as the product of the tissue density and wave propagation speed, as is portrayed in the following equation $Z = d \times c$, where Z is the acoustic impedance measured in kg/m^{2}s, d is the tissue density measured in kg/m^3, and c is the speed of the sound wave measured in meters per second (m/s).[52,53]

As its name suggests, impedance is the physical resistance that the acoustic waveform encounters as it passes through tissue. The image that is reconstructed is based on the degree of impedance in a specific tissue, as well as the difference in tissue impedance between consecutive tissues that the acoustic wave is penetrating. In terms of the degree of impedance, a dense tissue (e.g., bone) allows little wave absorption and instead strongly reflects the acoustic wave (Figure 2), resulting in a bright, white image.[53] In contrast, fluid such as blood, stomach gastric juice, and urine are not dense and primarily absorb the waveforms, resulting in darker images of the tissues/organs containing these fluids (blood vessels, stomach, and bladder, respectively). For this reason, fasted status has been suggested to potentially impact measurements of intra-abdominal structures[57] including adiposity.[58] In terms of the difference in impedance, if an acoustic wave is traveling through a tissue with a homogenous density, no interpretable image can be constructed, whereas waveforms that encounter a difference in impedance will result in a decipherable, well-contrasted image.[59] In other words, If two materials have the same acoustic impedance, their boundary will not produce an echo. If the difference in acoustic impedance is small, a weak echo will be produced, and most of the ultrasound waves will carry on and pass through the second medium. If the difference in acoustic impedance is large, a strong echo will be produced. If the difference in acoustic impedance is very large, the ultrasound waves will be entirely reflected. Typically, in soft tissues, the amplitude of an echo produced at a boundary is only a small percentage of the incident amplitudes, whereas areas containing bone or air can produce such large echoes that not enough ultrasound remains to image beyond the tissue interface. This principle is illustrated in Figure 2, with soft tissue producing a much greater echo compared to bone. Impedance is ultimately the primary variable that impacts the interaction of ultrasound waves with organs and tissues encountered along the ultrasound beam.

3.2.3 | Frequency and attenuation

Frequency is the number of wave cycles occurring per unit of time. Clinical ultrasound machines employ frequencies ranging from 1 to 15 MHz (1,000,000–15,000,000 Hz).[53] Higher frequencies correlate with shorter wavelengths, and vice versa. In soft tissue, the relationship between wavelength and frequency can be described by the following equation[55]:

$$\text{Wavelength (mm)} = 1.54\,\text{mm}/\text{frequency (MHz)}.$$

High frequencies and low wavelengths improve the high-axial image resolution by minimizing diffraction or the spread of the waveform.[55] In other words, increasing the number of waveforms and decreasing the wavelength enables more accurate discrimination between tissues of differing impedances, and thus improves image quality. However, compared to low-frequency waves, high-frequency waves more readily dissipate (lose wave amplitude and intensity), a phenomenon called attenuation.[53] Attenuation occurs due to a variety of factors including scattering, non-reciprocal wave reflection (mode conversion), and wave absorption, which is the most influential factor impacting attenuation.[55] Thus, high-frequency transducers (10–15 MHz) are optimal for imaging superficial structures (e.g., subcutaneous adiposity; 1–6 cm depth), whereas low-frequency transducers (2–5 MHZ) are preferred for imaging deep tissues. However, it is helpful to note that appropriate frequency may depend on how thick/how much body adiposity someone has; if someone is

leaner, a high-frequency transducer may still enable measurement of relatively deeper tissues. An example of attenuation in practice is that when acoustic echoes interact with high-density material such as bone, where the molecules are tightly packed together, attenuation is far greater than in adiposity, where the tissue molecules are less densely packed. This is because different tissues have different absorption coefficients,[53] with higher density materials having the capacity to absorb more of the acoustic signal, thus increasing attenuation to a greater extent than lower density materials, which do not absorb the same degree of signal.

4 | ULTRASOUND MEASUREMENT CONSIDERATIONS

This section will outline key methodological testing considerations for biomedical ultrasound use, including specific considerations for the measurement of central adiposity. These testing considerations include (i) transducer selection, (ii) image acquisition, (iii) subject preparation, (iv) image analysis, and (v) operator training. Familiarization with these considerations will enable optimal reporting of methods and results, and will better enable comparability across studies employing ultrasound-based measurements of central adiposity.

4.1 | Transducer selection

An ultrasound transducer is the component on the head of the probe which transmits and receives the acoustic sound waves produced by the machine. They come in a variety of shapes and sizes which impact a number of important factors including image resolution, field of view, penetration depth, and accessibility to specific anatomical locations/features. Thus, certain probes are often utilized for specified research and clinical purposes (e.g., pregnancy and fetal monitoring, mammograms, cardiac echocardiography, etc.). Importantly, most ultrasound machines can accommodate a variety of different probes, meaning one ultrasound device can perform a wide range of healthcare and research imaging applications.

Selection of the appropriate ultrasound transducer is primarily dependent on the required depth of penetration, image resolution, as well as the required field of view. Penetration depth is dependent on wavelength, where wavelength is the distance traveled by sound in one cycle. Lower frequency transducers (e.g., 2–5 MHz) have a longer wavelength and are thus able to penetrate more deeply but at the cost of image resolution. Higher-frequency probes (e.g., >10 MHz) produce smaller wavelengths, which provide better image resolution but at the cost of penetration depth. The frequency and type of transducer will affect the axial (sagittal) and lateral resolution of the reflected image. Axial resolution is the minimum distance that can be differentiated between two reflectors located parallel to the direction of ultrasound beam and is inversely proportional to the wavelength frequency. Lateral resolution is the minimum distance that can be distinguished between two reflectors located perpendicular to the direction of the ultrasound beam, and is affected by depth of imaging as well as the width of the beam. The desired field of view should determine the selection of either a linear array or curved array probe, with linear array transducers producing sound waves parallel to each other that result in a rectangular image. The width of the image is equal to the width of the probe (e.g., a 4-cm-wide probe will produce a 4-cm-wide image). Additionally, linear array transducers emit an equal number of scan lines at all penetration levels, ensuring consistent axial resolution. A narrow-width linear array, high-resolution (e.g., >10 MHz) transducer will ensure optimal near-field resolution. However, there are situations when a wider field of view is required such as during abdominal and pelvic diagnostic examinations.[54] Curved array probes produce a fan-like image, which is narrower near the transducer and increases in width with deeper penetration allowing for a greater field of view. With curved array transducers, the density of the scan lines decreases with increasing distance from the transducer, and the advantage of a greater field of view comes at the cost of lower lateral resolution.

An example in which a linear array probe would be used in the context of adiposity assessments would be for the assessment of maximum subcutaneous adiposity thickness (SFTmax; just above umbilicus, Figure 3). In this situation, a high-frequency, higher resolution (e.g., >10 MHz) linear array probe would allow adequate penetration and provide optimal (high) axial and lateral resolution. When imaging deeper sites such as during assessment of maximum preperitoneal adiposity thickness (PFT) and abdominal wall fat index (AFI), both of which are imaged below the xiphoid process (Figures 3 and 4), a medium-frequency (e.g., 5–10 MHz) linear array probe would typically be required, although a higher-frequency probe may be suitable if the individual was particularly lean in the abdominal region. Use of the medium-frequency linear array probe in this instance would help ensure adequate depth penetration while maintaining axial and lateral resolution. A scenario in which a curved array probe would be appropriate would be for a transverse plane assessment of intraabdominal adiposity thickness (IAT), a measure of intraperitoneal visceral adiposity (Figure 3). A curved array probe would ensure the linea alba and aorta appear in the same field of view. When imaging IAT, a low frequency (e.g., 2–5 MHz), curved array probe is required to ensure the sound waves can penetrate to the depth of the aorta, and that the linea alba and aorta can be seen in the same field of view. Lastly, the same transducer (and other operator settings such zoom, depth, etc.) should be maintained across subjects for a given study to maximize statistical power and minimize variability.

Additionally, ultrasound gel must be applied liberally to the aspect of the transducer which comes in contact with the skin.[52] Ultrasound gel provides lubrication which prevents the need for applying excess pressure on the probe and transducer, which could impact adiposity measurements by moving internal structures. More importantly, ultrasound waves dissipate rapidly in air because of the minimal impedance; ultrasound gel reduces the mismatch of acoustic impedance between air and skin tissue, and is thus used as medium to facilitate the transmission of the acoustic waves from the probe to the skin and vice versa.[60]

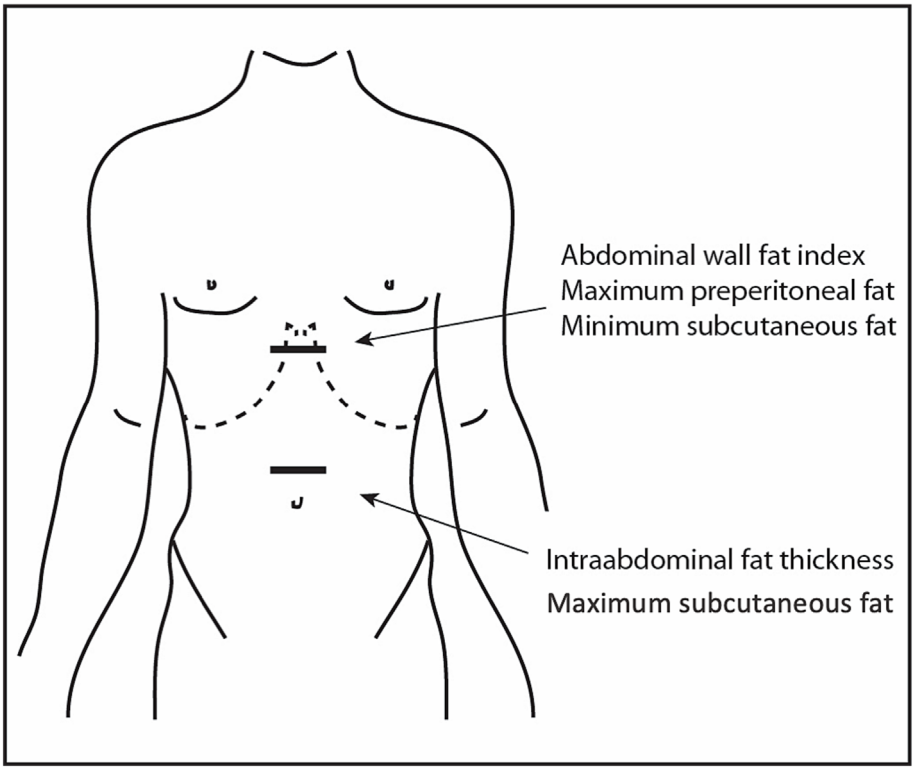

FIGURE 3 Anatomical locations of probe placement for measurements of intraabdominal adiposity thickness (IAT), abdominal wall fat index (AFI), maximum preperitoneal adiposity thickness, and minimum and maximum subcutaneous adiposity thickness measurements. IAT measurements are made 2 cm above the umbilicus at the xiphoumbilical line. AFI measurements are made immediately below the xiphoid process (epigastrium region). Figure was adapted from Stoner et al., 2015.[6]

4.2 | Image acquisition

Imaging procedures for central adiposity assessment conventionally utilize B-mode ultrasound with the echo amplitude distribution in a tomographic plane.[6,35] As mentioned earlier, ultrasound wave reflections will only have a prominent amplitude if they originate from acoustic interfaces with a marked change in impedance and are also oriented perpendicular (i.e., 90° angle) to the beam direction. For example, the anterior surface of the liver shows up distinctly, provided it is directly parallel to the transducer. Areas with low reflection amplitude, (e.g., internal contents of blood vessels) will be hypo-echoic and appear as blackish/dark gray. A related consideration for image acquisition is determining optimal probe orientation. For example, IAT (Figure 3) has been estimated as the thickness between the linea alba and the (1) spinal column (recommended; described in detail below), (2) anterior surface of the aorta, or (3) posterior surface of the aorta. If the aorta is being used for IAT measurements, the transverse view allows for both arterial walls to show up distinctly over a certain range provided that the arterial segment considered is straight and without branches. In contrast, in the sagittal view, the lateral segments of the artery wall are blurred, with relatively low amplitude for the anterior and posterior lumen-wall transitions. Thus, we recommend the transverse view for IAT measurements (described further below). As mentioned above, valid and reliable practice dictates that identical operator settings (e.g., zoom, depth, etc.), to the fullest extent possible, should be retained between and especially within subjects for any repeated or compared measurements to maximize statistical power and minimize variability.

4.3 | Subject preparation

Subject preparation guidelines are outlined in Table 2 and further discussed in this section. Consistency in subject posture and pre-assessment guidelines should be upheld in order to maximize internal validity and to optimize comparisons between studies.

Ideally, participants/patients should report to the laboratory or clinic hydrated so intra- and extra-cellular fluid shifts associated with dehydration do not alter the density of lean and adipose tissue. Individuals should also be tested in a fasted state. This may help to avoid abdominal swelling or bloating as well as changes in the true or on-screen size of adiposity depots.[58] However, fasting is not always feasible in certain clinical settings or with some special populations (i.e., pregnancy and diabetes) in which fasting may not be safe. Moderate and vigorous exercise should also be avoided for 24 h prior to testing, which may further assist in ensuring the subject is properly hydrated. It is also important to note that abdominal[61] bloating and fluid-volume shifts[62] associated with menstruation may theoretically alter central adipose tissue measurement results. Particularly for females, measuring at the same time of the month and recording the start date of their last menstrual cycle may be important considerations to take into account, although this may only be feasible for research and not clinical settings because of clinical healthcare settings often being limited by scheduling constraints and limited patient–practitioner availability. For both females and males, recording whether they are experiencing any bloating or abdominal swelling may be similarly important. However, further research is needed to determine whether females should be tested on certain days of their

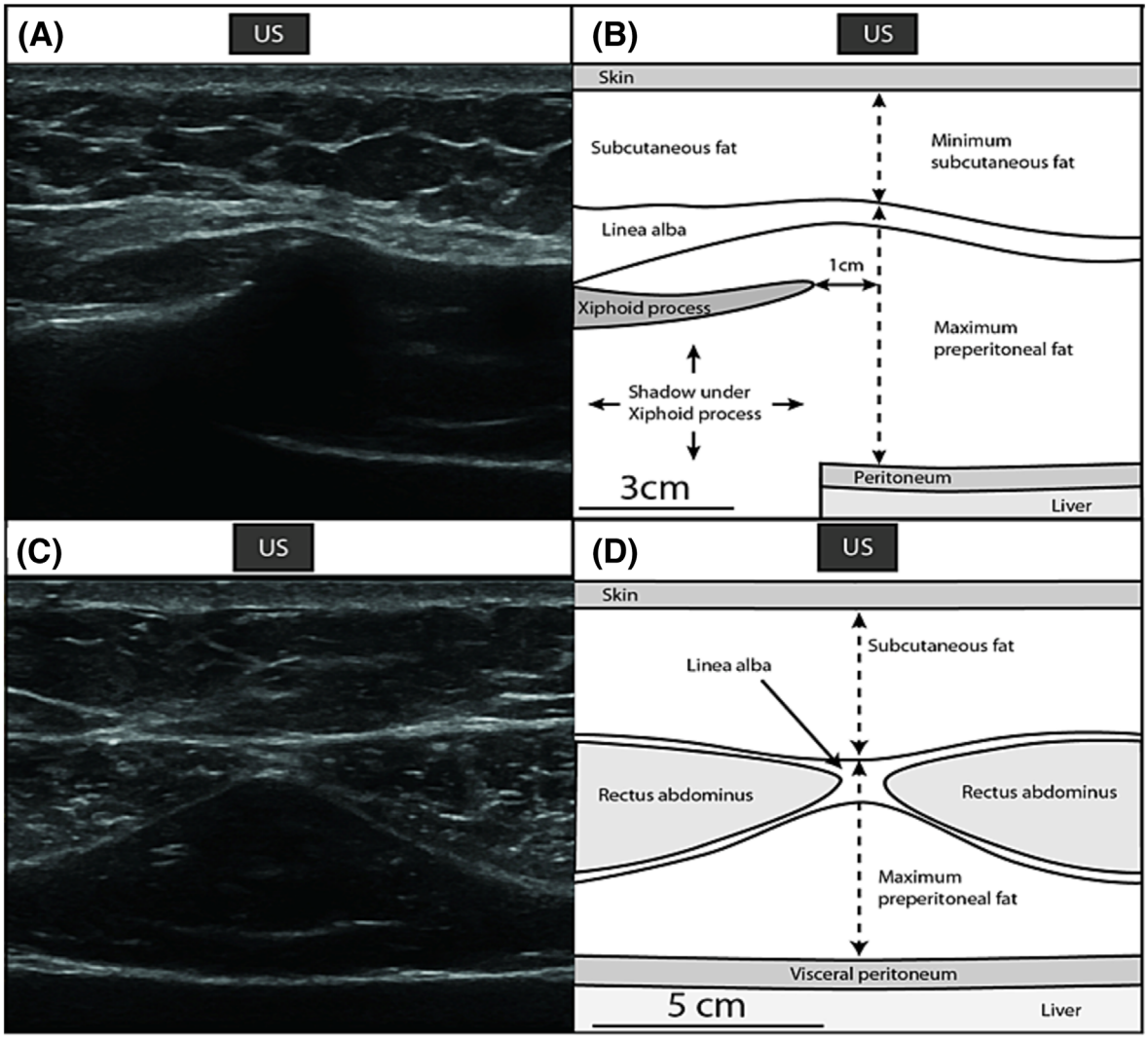

FIGURE 4 Ultrasound scans images (A, C) and corresponding schematic diagrams (B, D) for measurement of central adiposity. (A, B) Sagittal measurement of maximum preperitoneal adiposity thickness (sagittal plane). The ultrasound probe is placed immediately below the xiphoid process in the sagittal plane, with the measurement taking place 1 cm to the right of the xiphoid process. (C, D) Transverse measurement of maximum preperitoneal thickness (transverse plane). The ultrasound probe is placed immediately below the xiphoid process in the transverse plane. Abdominal wall fat index = maximum preperitoneal adiposity/minimum subcutaneous adiposity. Figure was adapted from Stoner et al., 2015.[6] cm; centimeters; US, ultrasound probe.

menstrual cycle. Like menstruation, circadian rhythm also impacts hormone levels[63] which may alter ultrasound-based adiposity measurements. Subjects returning for successive tests should be assessed at the same time of day to reduce variance associated with circadian rhythm variation (e.g., hormone shifts).

The participant should be lying supine after resting quietly for at least 10 min so that fluid-volume shifts between intra and extra-cellular compartments can stabilize. For image capture, approaches vary with some protocols having the participant resting their hands at their sides.[64] Based on our prior work,[6,46] and in-line with gold-standard CT[36] and MRI[45] assessments of central adiposity, we recommend having participants' hands places above their head and instructing them to exhale fully and hold their breath for 10 s. This approach minimizes variability associated with breathing-mediated changes in important measurement landmarks (e.g., aorta) as well as in the abdominal cavity's shape and volume generally. Ultimately, taking these considerations into account may increase the likelihood of producing valid and reliable measurements.

Because the chest cavity changes with breathing, we recommend capturing a 10-s video (most ultrasound machines have video-capture capabilities) rather than a still video capture for measurements. We recommend completing this process three times (i.e., three separate videos taken) and waiting 15–30 s between breath-holds and video captures to allow the participant to "catch" their breath and return to a comfortable, resting state. We recommend using the video clip to make three measurements (i.e., start, middle, and end), then calculating the average of the closest two measures.

TABLE 2 Guidelines for assessing intraabdominal adiposity thickness (IAT) and maximum preperitoneal adiposity thickness (PFT) with B-mode ultrasound. *Adapted from Stoner, 2016.*[6]

Parameter	Recommendations
Subject preparation	Ensure participant reports adequately hydrated and fasted to avoid abdominal swelling Avoid exercise during the preceding 24 h Women should be tested on day 1–7 of the menstrual cycle (i.e., day 7–14 of the ovarian cycle) Test conducted with subjects in the supine position Rest supine for at least 10 min in a quiet, temperature-controlled room at 21°C For successive tests, subjects should report at the same time of day to reduce error associated with circadian variation, for example, abdominal swelling
Probe selection	IAT: convex 6–1 MHz PFT: linear 15–7 MHz The same transducer should be used for all subjects in a given study
Ultrasound settings	Standardize global settings (acoustic output, gain, dynamic range, gamma, rejection).[53,54] Standardize probe-dependent settings (zoom factor, edge enhancement, frame averaging, and target frame rate).[53,54]
Probe placement	Little to no pressure should be used to avoid adiposity compression Scan transverse xiphoumbilical line IAT: 2 cm above the umbilicus PFT: immediately below the xiphoid process Place probe perpendicular to the skin, that is, avoid angling the probe Mark anatomical placement for studies with repeated measurements
Imaging	IAT: Posterior edge abdominal muscle (linea alba) to posterior surface of aorta. Ensure linea alba and aorta appear in the center of the image PFT: 1 cm to right of xiphoid process. Posterior edge abdominal muscle (linea alba) to anterior surface of the liver (peritoneum) Apply minimal pressure to avoid displacement of abdominal contents
Image capture	Participant holds hands over head Participant quietly expires and then holds breath to minimize chest movement Capture 10-s video while holding breath Measure during diastole, for 3 cardiac cycles
Image analysis	Extract three diastolic frames from video clip (for IAT, and only if aorta rather than vertebra used as measurement reference, though we recommend using vertebra) Use either integrated ultrasound unit software or video editing software (e.g., Avidemux, www.avidemux.org) to play clip, frame by frame, and identify diastole To make measurements, use caliper function with integrated ultrasound unit software or dedicated image processing application (e.g., ImageJ, http://imagej.nih.gov/ij) Note: a dedicated image processing application will enable off-site analysis and better enable multi-site collaboration
Operator	Operator training to ensure measurement reliability $n = 6$; within-day reliability (ICC ≥ 0.90; CV ≤ 5%) $n = 6$; between-day reliability (ICC ≥ 0.80, CV ≤ 5%) Same operator and analyst within study if possible to minimize between-operator variability If impossible to have only one operator/analyst Use same operator/analyst within the same participant (e.g., if multiple, longitudinal time points) $n = 6$; between-operator reliability (ICC ≥ 0.80, CV ≤ 5%)

Abbreviations: C, Celsius; cm, centimeters; CV, coefficient of variation; h, hours; IAT, intra-abdominal adiposity thickness; ICC, Intraclass correlation coefficient; MHz, megahertz; min, minutes; PFT, maximum preperitoneal adiposity thickness.

The aforementioned patient preparation guidelines are a conservative but feasible approach to minimize numerous sources of potential variance. However, the extent to which these factors impact ultrasound measures of central adiposity is unknown. For example, much of the considerations laid out above (e.g., fasted status, menstrual cycle phase, still image versus video captures) may or may not influence ultrasound measurements of central adiposity. Future research is needed to better understand the effects of pre-assessment guidelines and subject preparation considerations on ultrasound measurements of central adiposity. Doing so has the potential to reduce both participant/patient and researcher/clinician burden.

4.4 | Image analysis

Ultrasound measurements of central adiposity should ideally employ either integrated ultrasound unit software or external video editing software (e.g., Avidemux, www.avidemux.org; ImageJ, http://imagej.nih.gov/ij) with a caliper function in order to measure the distances between the landmarks specific to each adiposity index. Although we recommend using the anterior aspect of the vertebra as a reference point for IAT measurements, the participants/patients with obesity may require using the aorta if the vertebrae cannot be identified. In these cases in which the aorta is used as the landmark, editing

software and a gated electrocardiogram (ECG) will also need to identify diastole so that three diastolic frames can be extracted from the video clip. Following analysis of the three diastolic frames, the closest two measurements can be averaged. It should be noted that identifying three diastolic frames is not as important when measuring IAT using the vertebra as a landmark compared to the aorta; however, the chest cavity still changes with the cardiac cycle. Thus, using video-capture and ECG recordings offer the most conservative approach for IAT measurements (and other central adiposity measurements), regardless of which landmarks are being used. Additionally, a dedicated image processing application (e.g., Image J), as opposed to integrated ultrasound software, will enable off-site analysis and better enable multi-site collaboration because all sites can utilize the same analysis platform. Further, external image processing applications can give investigators greater flexibility to analyze videos at a time and place of their choosing (potentially expediting the analysis process), and most importantly, enabling the same analyzer(s) to process all video clips to minimize between-operator variability in analysis procedures.

Although automated techniques for assessing biomedical imaging of central adiposity have predominantly been conducted with MRI, CT, and DXA technology, preliminary research has also demonstrated that an automated ultrasound approach may be feasible and advantageous for assessments of central adiposity by being able to acceptably discriminate tissue boundaries.[52,65–67] For example, the MuscleSound® (Denver, Colorado, USA) software has been shown to be reliable (Intraclass correlation coefficient [ICC] = 0.997) and, despite being significantly different than DXA-based assessments of percent body adiposity (mean difference: 2.60 ± 1.32%), was highly correlated ($r = 0.93$, $p < 0.001$), and may be a promising approach for analyzing ultrasound-based measurements of central adiposity.[66] While additional work is needed to demonstrate the capacity of automated ultrasound imaging software to produce valid assessments of adiposity across different sites and adipose compartments, automated imaging techniques will offer advantages including increased objectivity, reduced human error, and minimized time burden.

4.5 | Operator training and related considerations

The sensitivity of ultrasound devices is such that subtle adjustments in probe position, angle, or pressure cause substantial changes in the image produced. Thus, operator training is essential in order to gain the fine motor skills and device familiarity necessary to produce reliable and valid measurements. In-person training with an experienced practitioner is recommended to achieve this consistency in user skill and performance. In terms of specific training benchmarks, each laboratory should establish a number (e.g., $n = 5–10$) of pilot participants to test for reliability in order to ensure operator skill and data quality. For example, our group typically employs pilot reliability sub-studies with at least $n = 6$. While $n = 6$ is not based on empirical evidence, it does support operator skill development and data quality. We recommend within-day (with measurements at least 10 min apart) reliability to have an ICC of ≥ 0.90, and between-day reliability of ICC ≥ 0.80.[68] If possible, the same operator should conduct all ultrasound measurements within a given study to minimize variance associated with between-operator differences. Similarly, if analysis is being conducted offline retrospectively, the same analyzer should perform all of the analysis within a given study (even if different than the ultrasound operator). However, we recognize that performing ultrasound measurements offline and/or by the same operator/analyst for a given patient may not be feasible in a clinical setting because of time and workflow constraints. If it is impossible to have only one operator/analyst (e.g., if multiple, longitudinal time points, multi-site study, etc.), between-operator (inter-rater) reliability of an ICC ≥ 0.80 should be achieved.[68]

5 | CENTRAL ADIPOSITY MEASUREMENTS: METHODOLOGICAL APPROACH

Despite improvements in the understanding and measurement of adiposity distribution, there is no global consensus as to the most important quantification or index of central adiposity, particularly in the context of ultrasound measurement. The measures described in the following subsections are some of the most commonly used ultrasound-based indices of central adiposity. These include measurements reflecting intra-abdominal adiposity including preperitoneal and visceral adiposity, subcutaneous adiposity, and the v/s ratio. Brief definitions of these measurements are included in Table 1, and details describing previously reported measurement protocols are outlined in Table 3, which has been included to help guide and standardize approaches for ultrasound measurements of central adiposity. Rationale for the specific measurement approaches described are also provided.

5.1 | Visceral (intraperitoneal) adiposity measures

5.1.1 | Intra-abdominal adiposity thickness

The primary marker of visceral adiposity is IAT and is sometimes referred to as visceral adipose tissue, visceral abdominal adiposity thickness, or abdominal adiposity thickness). IAT is the original ultrasound-derived indicator of visceral adiposity, first described by Armellini in 1990.[41] Although a number of anatomical measurement locations have been used (Tables 2 and 3), IAT is typically defined as the distance between either the anterior or posterior wall of the aorta and the linea alba (posterior surface of rectus abdominis muscle), measured 2 cm above the umbilicus at the xiphoumbilical line (transverse plane) (Figure 3). However, we recommend using the anterior aspect of the vertebra rather than the anterior or posterior aspect of the aorta as a landmark for IAT assessments because the greater density of the vertebra yields strong acoustic reflections and thus superior image clarity and consistency as a measurement landmark. It is most commonly measured using a convex/curved probe; although our group has also shown that in healthy adults with a range of somatotypes, the measurement can be conducted using a linear probe.[46]

TABLE 3 Comparison of protocols used to assess central adipose tissue.

Tissue	Acronym	Anatomical site	Measurement		Units	Probe	Orientation	Ref
			Site 1	Site 2				
Minimum subcutaneous thickness	SFT_{min}	Immediately ↓ xiphoid process	Adiposity–skin barrier	Anterior edge abdominal muscle (linea alba)	Dist.	Linear 12–5 MHz	Sagittal	4,28,69
		Immediately ↓ xiphoid process	Adiposity–skin barrier, 2-cm length	Anterior edge abdominal muscle (linea alba) 2-cm length	Area	Linear 12–5 MHz	Sagittal	69
		Upper median abdomen	Adiposity–skin barrier	Anterior edge abdominal muscle (linea alba)	Dist.	Convex 3.5 MHz	Sagittal	70
		Midpoint b/w xiphoid process and umbilicus	Posterior edge of abdominal muscles (linea alba)	Anterior edge abdominal muscle (linea alba)	Dist.	Linear 7.5 MHz	Transverse	21
Maximum preperitoneal thickness	PFT	Immediately ↓ xiphoid process	Posterior edge of abdominal muscles (linea alba)	Peritoneum (anterior surface of liver)	Dist.	Linear 12–5 MHz	Sagittal	4,28,42,69
		Immediately ↓ xiphoid process	Adiposity–skin barrier, 2-cm length	Anterior edge abdominal muscle (linea alba), 2-cm length	Area	Linear 12–5 MHz	Sagittal	69
		Upper median abdomen	Posterior edge of abdominal muscles (linea alba)	Peritoneum (anterior surface of liver)	Dist.	Convex 3.5 MHz	Sagittal	70
		Midpoint b/w xiphoid process and umbilicus	Posterior edge of abdominal muscles (linea alba)	Peritoneum	Dist.	Linear 7.5 MHz	Transverse	70
Preperitoneal circumference	PC	Midpoint b/w xiphoid process and umbilicus	Waist circumference – ($2\pi \times$ SFT)		Dist.	Linear 7.5 MHz	Transverse	21
Abdominal wall fat Index	AFI	Immediately ↓ xiphoid process	PFT/SFT_{min}		Ratio	Linear 12–7.5 MHz	Sagittal	4,28,42,69
		Immediately ↓ xiphoid process	PFT/SFT_{min} (using 2-cm length)		Ratio	Linear 12–5 MHz	Sagittal	69
		Upper median abdomen	PFT/SFT_{min}		Ratio	Convex 3.5 MHz	Sagittal	70
Maximum subcutaneous adiposity thickness	SFT_{max}	1–2 cm ↑umbilicus	Adiposity–skin barrier	Anterior edge abdominal muscle (linea alba)	Dist.	Linear 12–5 MHz	Sagittal	4,13,21,41,42
		1–3 cm ↑umbilicus	Adiposity–skin barrier	Anterior edge abdominal	Dist.	Convex 3.5 MHz	Transverse	36,37,40,70,71

(Continues)

TABLE 3 (Continued)

Tissue	Acronym	Anatomical site	Measurement		Units	Probe	Orientation	Ref
			Site 1	Site 2				
				muscle (linea alba)				
		Intercept xiphoid–waist	Adiposity–skin barrier	Anterior edge abdominal muscle (linea alba)	Dist.	Convex 3 MHz	Transverse	44
	SFT_{max}[B]	2 cm ↓umbilicus	Adiposity–skin barrier	Anterior edge abdominal muscle (linea alba)	Dist.	Linear 12.5 MHz	Sagittal	4
Intra-abdominal adiposity Thickness	IAT	1–5 cm ↑ umbilicus	Posterior edge of abdominal muscle (linea alba)	Anterior wall of the aorta	Dist.	Convex 5–2 MHz	Transverse	13,37,40–42,72
		1 cm ↑umbilicus	Posterior edge of abdominal muscles (linea alba)	Posterior wall of the aorta	Dist.	Convex 3.75–3.5 MHz	Transverse	36,39,72
		1–5 cm ↑umbilicus	Posterior edge of abdominal muscles (peritoneum)	Anterior edge lumbar vertebra or psoas muscle	Dist.	Convex 4–2 MHz	Transverse	4,7,12,34,70
		Intercept xiphoid–waist	Posterior edge of abdominal muscles (peritoneum)	Anterior edge lumbar vertebra or psoas muscle	Dist.	Convex 3 MHz	Sagittal	44
Maximum abdominal ratio	MAR	1 cm ↑umbilicus	IAT/SFT_{max}		Ratio	Convex 3.5 MHz	Transverse	37,40,70
		1 cm ↑umbilicus	IAT/SFT_{max}		Ratio	Convex 5–3.5 MHz Linear 12.5–5 MHz	Transverse/sagittal	4,42,72

Abbreviations: AFI, Abdominal wall fat index; b/w, between; cm, centimeters; dist, distance; IAT, intra-abdominal adiposity thickness; Min, minimum; MHz, megahertz; PC, preperitoneal circumference; PFT, maximum preperitoneal adiposity thickness; SFT_{max}, maximum subcutaneous adiposity thickness; SFT_{min}, minimum subcutaneous adiposity thickness; ↑, above; ↓, below.

These measurements had moderate–strong agreement with CT-[4,7,36,37,39,43] and MRI-[7,43] based measurements (r or ICC = 0.65–0.86). Moreover, IAT has been shown to have high intra-observer (ICC = 0.94–0.98, standard error of measurement [SEM]: 0.16–0.32 cm, minimum detectable change [MDC]: 0.43–0.88 cm; MDC%: 9.8–17.4%) and inter-observer (ICC: 0.97–1.00, SEM: 0.04–0.09 cm, MDC: 0.12–0.26 cm) reliabilities.[4,6,46]

In terms of clinical significance, IAT has been reported to be a significant marker of cardiovascular disease risk in both biological sexes.[39] Independent of age, biological sex, and BMI, IAT has also been found to be a significant predictor of the presence of metabolic syndrome,[12] as well as glucose intolerance in the later stages of pregnancy.[13] Using measurements made at the posterior aorta, cut-off values of 7 and 9 cm successfully differentiated males at moderate- and high-risk of cardiovascular disease, respectively, with corresponding values for females of 7 and 8 cm, respectively.[39] Further study is needed to determine appropriate cut-off points when measurements are conducted using the anterior aspect of the vertebral column (rather than aorta). Specific measurement and subject preparation guidelines for IAT are described in Tables 2 and 3.

5.2 | Visceral (preperitoneal) adiposity measures

5.2.1 | Maximum preperitoneal adiposity thickness

Like IAT, PFT is an index of visceral adiposity in the intra-abdominal region. However, whereas the IAT extends from the linea alba to the aorta or spine, the PFT extends from the linea alba to the anterior surface of the liver (left lobe) (Figure 4). PFT measurements are typically made by placing the probe immediately below the xiphoid process in the epigastrium region (Figures 3 and 4).[28] Measurements

have been made from both transverse and sagittal views, with both techniques indicating similarly acceptable reliability.[6] However, the sagittal view may facilitate easier operator training and may be the least prone to operator subjectivity given that the xiphoid process can be used as a clear landmark.[6] Ultrasound measurements have been positively correlated against those derived from CT (*r* or ICC = 0.75–0.87)[4,28,42] and are reliable, with high intra-observer (ICC = 0.91–0.98, SEM: 0.05 cm, MDC: 0.12–0.13 cm, MDC%: 7.1–7.5%) and inter-observer (ICC: 0.90–0.94, SEM: 0.03–0.04 cm, MDC: 0.09–0.10 cm, MDC%: 5.2–6.0%) reliabilities.[4,6] Measurement of PFT, however, seems to be a good alternative to calculation of AFI in lean persons, in whom higher values of AFI do not necessarily correspond to elevated cardiovascular disease risk.[19] PFT is elevated in patients with diabetes mellitus[73] and has been associated with disease severity, increased cardiovascular disease risk, and poor prognosis, as shown by the high prevalence of hypertension, microalbuminuria, retinopathy, and elevated levels of glycated hemoglobin (HbA1c).[73] PFT is also positively correlated with carotid intima-media thickness,[74] fasting insulin level,[74] triglyceride levels,[23,74] coronary arterial stenosis score,[23] fasting blood glucose level,[23] LDL, and total cholesterol levels.[23] It is negatively correlated with high-density lipoprotein cholesterol level in lean men. PFT measurement protocols are described in Tables 2 and 3.

5.3 | Subcutaneous adiposity measures

5.3.1 | Maximum subcutaneous adiposity

SFTmax is defined as the thickness of the subcutaneous adiposity between the anterior surface of linea alba and the adiposity–skin barrier, typically measured 2 cm above the umbilicus at the xiphoumbilical line (Figures 1 and 3). Ultrasound-derived SFTmax measurements are significantly correlated to CT-derived measurements (ICC = 0.95–0.96) and are reliable, with high intra- (ICC = 0.94–1.00, SEM: 0.06–0.10 cm, MDC: 0.17–0.25 cm, MDC%: 9.4–12.7%) and inter-observer (ICC: 0.88–1.00, SEM: 0.02–0.05 cm, MDC: 0.05–0.15 cm, MDC%: 3.0–9.1%) reliabilities.[4,6,46] At least one group[4] has attempted an alternative approach for estimating SFTmax, measuring 2 cm below instead of 2 cm above the umbilicus. Both the new and conventional measurement procedures yielded similar correlations to CT-derived measures (ICC = 0.96 vs ICC = 0.95, respectively), and similar intra- (ICC = 0.95 vs ICC = 0.99) and inter-observer (both ICC = 0.99) reliabilities.[4] SFTmax has been associated with coronary artery stenosis (in men only), LDL HDL, and total cholesterol.[23] Previously used SFTmax measurement protocols are described in Table 3.

5.3.2 | Minimum subcutaneous adiposity

Whereas SFTmax is defined as the thickness of subcutaneous adiposity between the linea alba and the adiposity–skin barrier, 2 cm above the umbilicus, minimum subcutaneous adiposity (SFTmin) is defined as the thickness of the subcutaneous adiposity between the anterior surface of linea alba and the adiposity–skin barrier measured just below the xiphoid process—a location with relatively little subcutaneous adiposity (Figures 1, 3, and 4). Measurements from ultrasound strongly correlate against those obtained from CT (ICC = 0.94, 95% CI: 0.89–0.97)[4] and have high intra- (ICC = 0.93–1.00, SEM: 0.03–0.04 cm, MDC: 0.07–0.10 cm, MDC%: 10.5–11.8%) and inter-observer reliabilities (ICC: 0.91–1.00, SEM: 0.02 cm, MDC: 0.05–0.06 cm, MDC%: 6.6–7.1%).[4,6,71]

In the limited number of studies in which it has been used, SFTmin has been associated with total cholesterol, LDL, and HDL, although not as strongly as PFT.[23] SFTmin has also been correlated with serum leptin levels.[73,75] Previously used SFTmin measurement protocols are described in Table 3.

5.4 | Visceral:subcutaneous adiposity ratio

5.4.1 | Abdominal wall fat index

AFI, first described by Suzuki in 1993[28] is the original v/s metric and is the ratio of PFT to SFTmin (Figures 3 and 4). Ultrasound-derived AFI measurements are significantly correlated to CT-derived measurements (ICC: 0.90, 95% CI: 0.82, 0.95) and are reliable, with high intra-observer (ICC = 0.90–1.00, SEM: 0.02 cm, MDC: 0.05–0.07 cm, MDC%13.8–14.4%) and inter-observer (ICC: 0.90–1.00, SEM: 0.02 cm, MDC: 0.04 cm, MDC%: 8.9–10.9%) reliabilities.[4,6] Although AFI can be measured in the transverse or sagittal plane, our group previously showed greater within-day reliability in the latter (reproducibility coefficients: 10.9% vs 8.9%, respectively).[6]

AFI is positively correlated with systolic blood pressure, diastolic blood pressure, triglycerides, total cholesterol, LDL, atherogenic index, and basal insulin levels in both biological sexes.[28,76] It is negatively correlated with HDL,[28] insulin sensitivity, and leptin levels in lean men, as well as in men with hyperlipidemia and obesity.[28,77,78] In men with obesity, AFI is inversely correlated with flow-mediated dilation,[79] the gold-standard indicator of endothelial function, and an early marker of CMD risk.[80] Higher ratios have corresponded to increased triglycerides, cholesterol, impaired glucose and lipid metabolism, and endothelial dysfunction..[19,28,79] Although AFI is a well-established index among persons with obesity, some studies have suggested that its diagnostic value is limited among lean, generally healthy individuals and those with diabetes.[23,73–75] In terms of diabetes, AFI has not had a significant correlation with insulin sensitivity, HDL, or carotid intima-media thickness in diabetic men or women.[42] In lean patients, the subcutaneous adiposity layer tends to be very thin, leading to abnormally high values of AFI and impairing its diagnostic accuracy.[74] In these cases, PFT is better correlated with metabolic[23] and cardiovascular disease risk factors.[23,74] Previously used AFI measurement protocols are described in Table 3.

5.4.2 | Maximum abdominal ratio

Whereas AFI is a v/s ratio of PFT:SFTmin, maximum abdominal ratio (MAR) is a v/s ratio of IAT:SFTmax. Ultrasound-derived MAR measurements are significantly correlated to CT-derived measurements (r or ICC = 0.57–0.89)[4,42] and are reliable, with high intra-observer (ICC = 0.83–1.00, SEM: <0.01–0.05 cm, MDC: 0.01–0.13 cm, MDC %: 13.2–26.8%) and inter-observer (ICC: 0.93–1.00, SEM: <0.01–0.03 cm, MDC: <0.01–0.08, MDC%: 6.3–14.6%) reliabilities.[4,6,46] At least one group[4] has calculated MAR by measuring SFTmax 2 cm below instead of 2 cm above the umbilicus, which did not result in appreciably different intra- ("above" ICC: 083–0.98 vs "below" ICC: 0.95–0.97) and inter-observer ("above" ICC: 0.96–0.98 vs "below" ICC: 0.93–0.99) reliabilities. However, as far as the authors are aware, there is an absence of clinical data to ascertain the value of the alternative MAR calculation. Few studies have specifically examined the associations between MAR and clinical outcomes. Previously used MAR measurement protocols are described in Table 3.

5.4.3 | Preperitoneal circumference

There are few current data that explore preperitoneal circumference (PC) as a clinical measurement index.[21] The PC is calculated as waist circumference—(2π × SFT), where SFT is measured at the midpoint between the umbilicus and the xiphoid process on the linea alba (e.g., not SFTmax or SFTmin). Thus, while PC is not a direct measure of the v/s ratio, it reflects the underlying construct of the v/s ratio by taking into account the subcutaneous adiposity component of the ratio (SFT) and an anthropometric substitute for the visceral component of the ratio (waist circumference). The PC has been found to be correlated with all of the components of metabolic syndrome (blood pressure, fasting blood glucose, triglycerides, high-density lipoproteins, and apolipoproteins A-1 and B levels) and with insulin resistance in healthy middle-aged volunteers,[21] and was more strongly associated with components of metabolic syndrome than SFT or waist circumferences independently.[21] Additional PC measurement details are described in Table 3.

6 | CLINICAL IMPLICATIONS

There are a number of relevant clinical implications for ultrasound-based measurement of central adiposity. In addition to the advantageous aspects of ultrasound mentioned previously (e.g., financially viable, no ionizing radiation, practical size, etc.), ultrasound is suitable for tracking longitudinal changes in central adiposity in interventions and epidemiological study designs. Ultrasound can also be used to measure vascular and hemodynamic variables such as blood flow, arterial calcification, endothelial function, arterial stiffness, and intima-media thickness to create a more comprehensive assessment of CMD risk via inspection of multiple physiological systems with a single device.[80] The fundamental utility of the technical and methodological information provided in this paper can also help researchers and clinicians ensure that ultrasound-based measurements of central adiposity are valid and reliable.

It is also important to note that the robust methodological detail provided in this paper offers a preliminary framework that health-care practitioners may eventually implement to make superior clinical decisions using ultrasound as compared to BMI, the most common, yet intrinsically flawed marker of obesity status because of its inability to differentiate adiposity versus lean mass. For example, BMI measurements among children—a population of great interest in the context of body composition given concerning rates of childhood obesity[81]—have been poorly correlated with ultrasound-derived SFT, underscoring that individuals with identical BMI's can have large differences in their quantity and distribution of adipose tissue (in children, > 2–3 fold).[82] In terms of overt CMD risk prediction, compared to anthropometric indices that reflect but do not measure body composition, ultrasound-based measures of IAT and SFT are more strongly related to components of metabolic syndrome including systolic blood pressure, total cholesterol, and low-density lipoprotein in obese diabetics and non-obese non-diabetics.[83] Notably, the feasibility and superior use of ultrasound-based prediction of CMD risk factors have also been demonstrated in clinical settings. In a Metabolic Disorders Clinic in Italy, ultrasound-derived assessments of IAT outperformed BMI in terms of predicting intima-media thickness, Framingham Risk score, and vascular age.[84] Collectively, ultrasound-based assessments of central adiposity can offer important, and compared to anthropometry, often superior reflections of CMD risk in a variety of populations and within both research and clinical settings.

7 | CONCLUSION

Ultrasound is a safe and relatively inexpensive technology that can be utilized for assessing central adiposity. In this paper, we have described the main depots of central adiposity along with the pathophysiological importance of these depots in the context of CMD risk. We have also outlined the key components of ultrasound, both in terms of the history of the technology as well as the physics involved in measurement. Additionally, we have described the clinical relevance of several of the most common ultrasound-based measurements of adiposity including indices of visceral (both intraperitoneal and preperitoneal) and subcutaneous adiposity, as well as the v/s ratio. Moreover, we have provided recommendations for the specific approaches that may be used for these measurements and have offered rationale to support these recommendations. By highlighting these key technical and clinical components, we hope to provide users with the practical tools and understanding necessary to support the acquisition of valid and reliable ultrasound-based measurements of central adiposity. Future research is needed to further develop standard protocols as well as to determine a gold-standard index of ultrasound-based central adiposity, particularly in the context of reflecting CMD risk.

ACKNOWLEDGMENTS

None.

CONFLICT OF INTEREST STATEMENT

The authors have no conflict of interest to declare.

ORCID

Gabriel Zieff https://orcid.org/0000-0002-4043-2911

REFERENCES

1. Shuster A, Patlas M, Pinthus JH, Mourtzakis M. The clinical importance of visceral adiposity: a critical review of methods for visceral adipose tissue analysis. *Br J Radiol*. 2012;85(1009):1-10. doi:10.1259/bjr/38447238
2. Fox CS, Massaro JM, Hoffmann U, et al. Abdominal visceral and subcutaneous adipose tissue compartments: association with metabolic risk factors in the Framingham heart study. *Circulation*. 2007;116(1):39-48. doi:10.1161/CIRCULATIONAHA.106.675355
3. Peiris AN, Sothmann MS, Hoffmann RG, et al. Adiposity, fat distribution, and cardiovascular risk. *Ann Intern Med*. 1989;110(11):867-872. doi:10.7326/0003-4819-110-11-867
4. Bazzocchi A, Filonzi G, Ponti F, et al. Accuracy, reproducibility and repeatability of ultrasonography in the assessment of abdominal adiposity. *Acad Radiol*. 2011;18(9):1133-1143. doi:10.1016/J.ACRA.2011.04.014
5. Owens S, Gutin B, Ferguson M, Allison J, Karp W, Le NA. Visceral adipose tissue and cardiovascular risk factors in obese children. *J Pediatr*. 1998;133(1):41-45. doi:10.1016/S0022-3476(98)70175-1
6. Stoner L, Chinn V, Cornwall J, et al. Reliability tests and guidelines for B-mode ultrasound assessment of central adiposity. *Eur J Clin Invest*. 2015;45(11):1200-1208. doi:10.1111/eci.12540
7. Stolk RP, Wink O, Zelissen PMJ, Meijer R, Van Gils APG, Grobbee DE. Validity and reproducibility of ultrasonography for the measurement of intra-abdominal adipose tissue. *Int J Obes (Lond)*. 2001;25(9):1346-1351. doi:10.1038/sj.ijo.0801734
8. Ouchi N, Parker JL, Lugus JJ, Walsh K. Adipokines in inflammation and metabolic disease. *Nat Rev Immunol*. 2011;11(2):85-97. doi:10.1038/nri2921
9. Kalra A, Wehrle CJ, Tuma F. Anatomy, abdomen and pelvis, peritoneum. *StatPearls*. July 2022. Accessed December 28, 2022. https://www.ncbi.nlm.nih.gov/books/NBK534788/
10. Bergman RN, Kim SP, Catalano KJ, et al. Why visceral fat is bad: mechanisms of the metabolic syndrome. *Obesity (Silver Spring)*. 2006;14(S2):1. doi:10.1038/OBY.2006.277
11. Björntorp P. Metabolic implications of body fat distribution. *Diabetes Care*. 1991;14(12):1132-1143. doi:10.2337/DIACARE.14.12.1132
12. Stolk RP, Meijer R, Mali WP, Grobbee DE, van der Graaf Y, Secondary Manifestations of Arterial Disease Study G. Ultrasound measurements of intraabdominal fat estimate the metabolic syndrome better than do measurements of waist circumference. *Am J Clin Nutr*. 2003;77(4):857-860. doi:10.1093/ajcn/77.4.857
13. Martin AM, Berger H, Nisenbaum R, et al. Abdominal visceral adiposity in the first trimester predicts glucose intolerance in later pregnancy. *Diabetes Care*. 2009;32(7):1308-1310. doi:10.2337/DC09-0290
14. Philipsen A, Jørgensen ME, Vistisen D, et al. Associations between ultrasound measures of abdominal fat distribution and indices of glucose metabolism in a population at high risk of type 2 diabetes: the ADDITION-PRO study. *PLoS ONE*. 2015;10(4):e0123062. doi:10.1371/JOURNAL.PONE.0123062
15. Trayhurn P, Wood IS. Adipokines: inflammation and the pleiotropic role of white adipose tissue. *Br J Nutr*. 2004;92(3):347-355. doi:10.1079/BJN20041213
16. Kin HL, Yu LC, Wing BC, Chan JCN, Chu CWW. Mesenteric fat thickness is an independent determinant of metabolic syndrome and identifies subjects with increased carotid intima-media thickness. *Diabetes Care*. 2006;29(2):379-384. doi:10.2337/DIACARE.29.02.06.DC05-1578
17. Hanlon CL, Yuan L. Nonalcoholic fatty liver disease: the role of visceral adipose tissue. *Clin Liver Dis*. 2022;19(3):106-110. doi:10.1002/CLD.1183
18. Ahima RS, Flier JS. Adipose tissue as an endocrine organ. *Trends Endocrinol Metab*. 2000;11(8):327-332. doi:10.1016/S1043-2760(00)00301-5
19. Vlachos IS, Hatziioannou A, Perelas A, Perrea DN. Sonographic assessment of regional adiposity. *Am J Roentgenol*. 2007;189(6):1545-1553. doi:10.2214/AJR.07.2366
20. Sabir N, Pakdemirli E, Sermez Y, Zencir M, Kazil S. Sonographic assessment of changes in thickness of different abdominal fat layers in response to diet in obese women. *J Clin Ultrasound*. 2003;31(1):26-30. doi:10.1002/jcu.10129
21. Meriño-Ibarra E, Artieda M, Cenarro A, et al. Ultrasonography for the evaluation of visceral fat and the metabolic syndrome. *Metabolism*. 2005;54(9):1230-1235. doi:10.1016/J.METABOL.2005.04.009
22. Miyazaki R, Hoka S, Yamaura K. Visceral fat, but not subcutaneous fat, is associated with lower core temperature during laparoscopic surgery. *PLoS ONE*. 2019;14(6):e0218281. doi:10.1371/JOURNAL.PONE.0218281
23. Tadokoro N, Murano S, Nishide T, et al. Preperitoneal fat thickness determined by ultrasonography is correlated with coronary stenosis and lipid disorders in non-obese male subjects. *Int J Obes (Lond)*. 2000;24(4):502-507. doi:10.1038/sj.ijo.0801187
24. Cuatrecasas G, de Cabo F, Coves MJ, et al. Ultrasound measures of abdominal fat layers correlate with metabolic syndrome features in patients with obesity. *Obes Sci Pract*. 2020;6(6):660-667. doi:10.1002/OSP4.453
25. Porter SA, Massaro JM, Hoffmann U, Vasan RS, O'Donnel CJ, Fox CS. Abdominal subcutaneous adipose tissue: a protective fat depot? *Diabetes Care*. 2009;32(6):1068-1075. doi:10.2337/DC08-2280
26. Ravussin E, Smith SR. Increased fat intake, impaired fat oxidation, and failure of fat cell proliferation result in ectopic fat storage, insulin resistance, and type 2 diabetes mellitus. *Ann N Y Acad Sci*. 2002;967(1):363-378. doi:10.1111/J.1749-6632.2002.TB04292.X
27. Booth AD, Magnuson AM, Fouts J, et al. Subcutaneous adipose tissue accumulation protects systemic glucose tolerance and muscle metabolism. *Adipocyte*. 2018;7(4):261-272. doi:10.1080/21623945.2018.1525252
28. Suzuki R, Watanabe S, Hirai Y, et al. Abdominal wall fat index, estimated by ultrasonography, for assessment of the ratio of visceral fat to subcutaneous fat in the abdomen. *Am J Med*. 1993;95(3):309-314. doi:10.1016/0002-9343(93)90284-V
29. Fujimoto WY, Bergstrom RW, Boyko EJ, et al. Visceral adiposity and incident coronary heart disease in Japanese-American men. The 10-year follow-up results of the Seattle Japanese-American community diabetes study. *Diabetes Care*. 1999;22(11):1808-1812. doi:10.2337/DIACARE.22.11.1808
30. Kannel WB. Lipids, diabetes, and coronary heart disease: insights from the Framingham study. *Am Heart J*. 1985;110(5):1100-1107. doi:10.1016/0002-8703(85)90224-8
31. Wei M, Gaskill SP, Haffner SM, Stern MP. Waist circumference as the best predictor of noninsulin dependent diabetes mellitus (NIDDM) compared to body mass index, waist/hip ratio and other anthropometric measurements in Mexican Americans—a 7-year prospective study. *Obes Res*. 1997;5(1):16-23. doi:10.1002/J.1550-8528.1997.TB00278.X
32. Bonora E, Micciolo R, Ghiatas AA, et al. Is it possible to derive a reliable estimate of human visceral and subcutaneous abdominal adipose

tissue from simple anthropometric measurements? *Metabolism*. 1995; 44(12):1617-1625. doi:10.1016/0026-0495(95)90084-5
33. Wajchenberg BL. Subcutaneous and visceral adipose tissue: their relation to the metabolic syndrome. *Endocr Rev*. 2000;21(6):697-738. doi:10.1210/EDRV.21.6.0415
34. Tornaghi G, Raiteri R, Pozzato C, et al. Anthropometric or ultrasonic measurements in assessment of visceral fat? A comparative study. *Int J Obes Relat Metab Disord*. 1994;18(11):771-775.
35. Abe T, Kawakami Y, Sugita M, Yoshikawa K, Fukunaga T. Use of B-mode ultrasound for visceral fat mass evaluation: comparisons with magnetic resonance imaging. *Appl Human Sci*. 1995;14(3):133-139. doi:10.2114/AHS.14.133
36. Pontiroli AE, Pizzocri P, Giacomelli M, et al. Ultrasound measurement of visceral and subcutaneous fat in morbidly obese patients before and after laparoscopic adjustable gastric banding: comparison with computerized tomography and with anthropometric measurements. *Obes Surg*. 2002;12(5):648-651. doi:10.1381/096089202321019620
37. Ribeiro-Filho FF, Faria AN, Azjen S, Zanella MT, Ferreira SRG. Methods of estimation of visceral fat: advantages of ultrasonography. *Obes Res*. 2003;11(12):1488-1494. doi:10.1038/OBY.2003.199
38. Cigolini M, Targher G, Andreis IAB, Tonoli M, Agostino G, De Sandre G. Visceral fat accumulation and its relation to plasma hemostatic factors in healthy men. *Arterioscler Thromb Vasc Biol*. 1996; 16(3):368-374. doi:10.1161/01.ATV.16.3.368
39. Leite CC, Wajchenberg BL, Radominski R, Matsuda D, Cerri GG, Halpern A. Intra-abdominal thickness by ultrasonography to predict risk factors for cardiovascular disease and its correlation with anthropometric measurements. *Metabolism*. 2002;51(8):1034-1040. doi:10.1053/META.2002.34035
40. Ribeiro-Filho FF, Faria AN, Kohlmann O, et al. Ultrasonography for the evaluation of visceral fat and cardiovascular risk. *Hypertension*. 2001;38(3 Pt 2):713-717. doi:10.1161/01.HYP.38.3.713
41. Armellini F, Zamboni M, Rigo L, et al. The contribution of sonography to the measurement of intra-abdominal fat. *J Clin Ultrasound*. 1990; 18(7):563-567. doi:10.1002/jcu.1870180707
42. Kim SK, Kim HJ, Hur KY, et al. Visceral fat thickness measured by ultrasonography can estimate not only visceral obesity but also risks of cardiovascular and metabolic diseases. *Am J Clin Nutr*. 2004;79(4): 593-599. doi:10.1093/ajcn/79.4.593
43. Iacobellis G, Assael F, Ribaudo MC, et al. Epicardial fat from echocardiography: a new method for visceral adipose tissue prediction. *Obes Res*. 2003;11(2):304-310. doi:10.1038/OBY.2003.45
44. De Lucia Rolfe E, Sleigh A, Finucane FM, et al. Ultrasound measurements of visceral and subcutaneous abdominal thickness to predict abdominal adiposity among older men and women. *Obesity*. 2010; 18(3):625-631. doi:10.1038/OBY.2009.309
45. Iacobellis G, Ribaudo MC, Assael F, et al. Echocardiographic epicardial adipose tissue is related to anthropometric and clinical parameters of metabolic syndrome: a new indicator of cardiovascular risk. *J Clin Endocrinol Metab*. 2003;88(11):5163-5168. doi:10.1210/JC.2003-030698
46. Stoner L, Geoffron M, Cornwall J, et al. Reliability of central adiposity assessments using B-mode ultrasound: a comparison of linear and curved array transducers. *Ultrasound Q*. 2016;32(4):342-348. doi:10.1097/RUQ.0000000000000256
47. The History of Ultrasound|BMUS. Accessed July 15, 2022. https://www.bmus.org/for-patients/history-of-ultrasound/
48. Donald I, Macvicar J, Brown TG. Investigation of abdominal masses by pulsed ultrasound. *Lancet*. 1958;271(7032):1188-1195. doi:10.1016/S0140-6736(58)91905-6
49. Global Ultrasound Device Market Size Report 2022-2030. Accessed July 15, 2022. https://www.grandviewresearch.com/industry-analysis/ultrasound-device-market
50. Wagner DR, Thompson BJ, Anderson DA, Schwartz S. A-mode and B-mode ultrasound measurement of fat thickness: a cadaver validation study. *Eur J Clin Nutr*. 2018;73(4):518-523. doi:10.1038/s41430-018-0085-2
51. Lloyd T, Tang YM, Benson MD, King S. Diaphragmatic paralysis: the use of M mode ultrasound for diagnosis in adults. *Spinal Cord*. 2006; 44(8):505-508. doi:10.1038/sj.sc.3101889
52. Wagner DR. Ultrasound as a tool to assess body fat. *J Obes*. 2013; 2013:280713. doi:10.1155/2013/280713
53. Abu-Zidan FM, Hefny AF, Corr P. Clinical ultrasound physics. *J Emerg Trauma Shock*. 2011;4(4):501-503. doi:10.4103/0974-2700.86646
54. Bakhru RN, Schweickert WD. Intensive care ultrasound: I. Physics, equipment, and image quality. *Ann am Thorac Soc*. 2013;10(5):540-548. doi:10.1513/AnnalsATS.201306-191OT
55. Kremkau F. *Sonography principles and instruments*. 9th ed. Saunders; 2016.
56. Thrush A, Hartshorne Ti. *Vascular ultrasound: How, why and when*. 3rd ed. 2010.
57. Ehrenstein BP, Froh S, Schlottmann K, Schlmerich J, Schacherer D. To eat or not to eat? Effect of fasting prior to abdominal sonography examinations on the quality of imaging under routine conditions: a randomized, examiner-blinded trial. *Scand J Gastroenterol*. 2009;44(9): 1048-1054. doi:10.1080/00365520903075188
58. Philipsen A, Carstensen B, Sandbaek A, Almdal TP, Johansen NB, Witte DR. Reproducibility of ultrasonography for assessing abdominal fat distribution in a population at high risk of diabetes. *Nutr Diabetes*. 2013;3(8):e82. doi:10.1038/nutd.2013.23
59. Chan V, Perlas A. Basics of ultrasound imaging. In: *Atlas of ultrasound-guided procedures in interventional pain management*; 2011. doi:10.1007/978-1-4419-1681-5_2
60. Afzal S, Zahid M, Rehan ZA, et al. Preparation and evaluation of polymer-based ultrasound gel and its application in ultrasonography. *Gels*. 2022;8(1):42. doi:10.3390/GELS8010042
61. Biggs WS. Premenstrual syndrome and premenstrual dysphoric disorder. 2011; 84. Accessed December 29, 2022. www.aafp.org/afp
62. Rosenfeld R, Livne D, Nevo O, et al. Hormonal and volume dysregulation in women with premenstrual syndrome. *Hypertens (Dallas, Tex 1979)*. 2008;51(4):1225-1230. doi:10.1161/HYPERTENSIONAHA.107.107136
63. Gnocchi D, Bruscalupi G. Circadian rhythms and hormonal homeostasis: pathophysiological implications. *Biology (Basel)*. 2017;6(1):10. doi:10.3390/BIOLOGY6010010
64. Asano T, Kubota N, Koizumi N, et al. Novel and simple ultrasonographic methods for estimating the abdominal visceral fat area. *Int J Endocrinol*. 2017;2017:8796069. doi:10.1155/2017/8796069
65. Green JJ, Smith RW, Stratton MT, et al. Cross-sectional and longitudinal associations between subcutaneous adipose tissue thickness and dual-energy X-ray absorptiometry fat mass. *Clin Physiol Funct Imaging*. 2021;41(6):514-522. doi:10.1111/CPF.12727
66. Bradley AP, Klawitter L, Carver E, et al. Reliability of a novel automated ultrasound technology for body composition assessment and comparisons with dual energy X-ray absorptiometry. *Int J Exerc Sci*. 2023;16(4):393-401.
67. Inoue M, Bu N, Fukuda O, Okumura H. Automated discrimination of tissue boundaries using ultrasound images of "ubiquitous echo". *Annu Int Conf IEEE Eng Med Biol Soc IEEE Eng Med Biol Soc Annu Int Conf* 2007;2007:1330–1334. doi:10.1109/IEMBS.2007.4352543
68. Koo TK, Li MY. A guideline of selecting and reporting Intraclass correlation coefficients for reliability research. *J Chiropr Med*. 2016;15(2): 155-163. doi:10.1016/j.jcm.2016.02.012
69. Holzhauer S, Zwijsen RML, Jaddoe VWV, et al. Sonographic assessment of abdominal fat distribution in infancy. *Eur J Epidemiol*. 2009; 24(9):521-529. doi:10.1007/s10654-009-9368-1
70. Koda M, Senda M, Kamba M, Kimura K, Murawaki Y. Sonographic subcutaneous and visceral fat indices represent the distribution of body fat volume. *Abdom Imaging*. 2007;32(3):387-392. doi:10.1007/S00261-006-9082-3/TABLES/1

71. Bellisari A, Roche AF, Siervogel RM. Reliability of B-mode ultrasonic measurements of subcutaneous adipose tissue and intra-abdominal depth: comparisons with skinfold thicknesses. *Int J Obes Relat Metab Disord*. 1993;17(8):475-480.
72. Armellini F, Zamboni M, Rigo L, et al. Sonography detection of small intra-abdominal fat variations. *Int J Obes (Lond)*. 1991;15(12):847-852.
73. Tayama K, Inukai T, Shimomura Y. Preperitoneal fat deposition estimated by ultrasonography in patients with non-insulin-dependent diabetes mellitus. *Diabetes Res Clin Pract*. 1999;43(1):49-58. doi:10.1016/S0168-8227(98)00118-1
74. Yamamoto M, Egusa G, Hara H, Yamakido M. Association of intraabdominal fat and carotid atherosclerosis in non-obese middle-aged men with normal glucose tolerance. *Int J Obes (Lond)*. 1997;21(10):948-951. doi:10.1038/sj.ijo.0800501
75. Shimizu H, Shimomura Y, Hayashi R, et al. Serum leptin concentration is associated with total body fat mass, but not abdominal fat distribution. *Int J Obes (Lond)*. 1997;21(7):536-541. doi:10.1038/SJ.IJO.0800437
76. Kawamoto R, Kajiwara T, Oka Y, Takagi Y. Association between abdominal wall fat index and carotid atherosclerosis in women. *J Atheroscler Thromb*. 2002;9(5):213-218. doi:10.5551/jat.9.213
77. Kondo I, Mizushige K, Hirao K, et al. Ultrasonographic assessment of coronary flow reserve and abdominal fat in obesity. *Ultrasound Med Biol*. 2001;27(9):1199-1205. doi:10.1016/S0301-5629(01)00427-6
78. Soyama A, Nishikawa T, Ishizuka T, et al. Clinical usefulness of the thickness of preperitoneal and subcutaneous fat layer in the abdomen estimated by ultrasonography for diagnosing abdominal obesity in each type of impaired glucose tolerance in man. *Endocr J*. 2005;52(2):229-236. doi:10.1507/ENDOCRJ.52.229
79. Hashimoto M, Akishita M, Eto M, et al. The impairment of flow-mediated vasodilatation in obese men with visceral fat accumulation. *Int J Obes (Lond)*. 1998;22(5):477-484. doi:10.1038/SJ.IJO.0800620
80. Stoner L, Sabatier MJ. Use of ultrasound for non-invasive assessment of flow-mediated dilation. *J Atheroscler Thromb*. 2012;19(5):407-421. doi:10.5551/jat.11395
81. Jankowska A, Brzezí Nski M, Romanowicz-Sołtyszewska A, Szlagatys-Sidorkiewicz A. Metabolic syndrome in obese children-clinical prevalence and risk factors. *Int J Environ Res Public Heal Artic Public Heal*. 2021;18:1060. doi:10.3390/ijerph
82. Schmid-Zalaudek K, Brix B, Sengeis M, et al. Subcutaneous adipose tissue measured by b-mode ultrasound to assess and monitor obesity and cardio–metabolic risk in children and adolescents. *Biology (Basel)*. 2021;10(5):449. doi:10.3390/BIOLOGY10050449/S1
83. Premanath M, Basavanagowdappa H, Mahesh M, Suresh M. Correlation of abdominal adiposity with components of metabolic syndrome, anthropometric parameters and insulin resistance, in obese and non obese, diabetics and non diabetics: a cross sectional observational study. (Mysore visceral adiposity in diabetes study). *Indian J Endocrinol Metab*. 2014;18(5):676-682. doi:10.4103/2230-8210.139231
84. Bellan M, Menegatti M, Ferrari C, Carnevale Schianca GP, Pirisi M. Ultrasound-assessed visceral fat and associations with glucose homeostasis and cardiovascular risk in clinical practice. *Nutr Metab Cardiovasc Dis*. 2018;28(6):610-617. doi:10.1016/J.NUMECD.2018.01.006

How to cite this article: Zieff G, Cornwall J, Blue MN, Smith-Ryan AE, Stoner L. Ultrasound-based measurement of central adiposity: Key considerations and guidelines. *Obesity Reviews*. 2024;e13716. doi:10.1111/obr.13716